No effect of thermal maturity on the Mo-, U-, Cd- and Zn-isotope compositions of Lower Jurassic organic-rich sediments

Alexander J. Dickson[1,2]*, Erdem Idiz[1], Don Porcelli[1], Melissa J. Murphy[1], Ricardo Celestino[3], Hugh C. Jenkyns[1], Simon W. Poulton[4], Stephen P. Hesselbo[3], John N. Hooker[1,5], Micha Ruhl[1,6], Sander H.J.M. van den Boorn[7]

1. Department of Earth Sciences, University of Oxford, Oxford, OX1 3AN, UK
2. Department of Earth Sciences, Royal Holloway University of London, Surrey, TW20 0EX, UK
3. Camborne School of Mines, University of Exeter, Penryn, Cornwall, TR10 9FE, UK
4. School of Earth and Environment, University of Leeds, Leeds, LS2 9JT, UK
5. School of Mathematics, Science and Engineering, University of the Incarnate Word, San Antonio, Texas 78209, USA
6. Department of Geology, Trinity College Dublin, The University of Dublin, Dublin 2, Ireland
7. Shell Global Solutions International B.V., Grasweg 31, 1031 HW Amsterdam, The Netherlands

*Corresponding author: alex.dickson@rhul.ac.uk

ABSTRACT

The isotope ratios of redox-sensitive metals in organic-rich rocks are critical tools for quantifying the timing and severity of deoxygenation and nutrient cycling in Earth's past. The resilience of isotopic data to thermal alteration of the host sediments over millions of years of burial is, however, largely unknown. Here we present Mo, U, Cd and Zn stable-isotope data from two stratigraphic successions of the same Lower Jurassic Posidonienschiefer unit in the Lower Saxony Basin of North Germany that were affected by different burial histories. We show that thermal maturity had no effect on the isotopic compositions of these elements but does appear to have increased their concentrations in the rock. The data corroborate the results of laboratory-based maturation studies and provide constraints on the Mo-, U-, Cd- and Zn- isotopic compositions of ~182 Ma seawater in the Lower Saxony Basin.

INTRODUCTION

Isotopic measurements of metallic elements are widely employed as a means to elucidate the redox history of the oceans. Some elements, such as molybdenum (Mo) and uranium (U), have been used to trace the development of oxygenated conditions on Earth, and to quantify the expansion and contraction of deoxygenated zones in the oceans (Dickson, 2017; Clarkson et al., 2018). The isotopic compositions of several other metals, including zinc (Zn) and cadmium (Cd), might also record redox conditions or productivity, due to their strong affinity for burial in organic-rich sediments (Little et al., 2016; Vance et al., 2016; Isson et al., 2018; Bryan et al., 2021). However, the application of these latter two isotope systems to disentangle paleo-chemical changes in the oceans is still in its infancy (e.g. Georgiev et al., 2015; Sweere et al., 2020).

An important prerequisite for the robust application of any paleo-environmental proxy is that the mineral or sedimentary archive used to infer past chemical conditions was unaffected

by diagenetic or metamorphic processes; or at least that the effect of such processes on the measured chemical composition can be quantified (Eroglu et al., 2021). Catagenesis (thermal maturation of organic matter) may have a central role to play in altering the geochemical signature of metals at high burial temperatures due to metal adsorption onto, and incorporation into, organic molecules (Lewan and Maynard, 1982; Chappaz et al., 2014; Dahl et al., 2017). However, the effect of catagenesis on metal isotopes in a widely employed paleo-chemical archive, namely organic-rich shales, is not well understood.

GEOLOGICAL SETTING

The Lower Saxony Basin (LSB) in northern Germany (Fig. 1) preserves an ~182 Ma organic-rich unit called the Posidonienschiefer. Since its formation in the Early Jurassic, this unit has been buried to a variety of depths within the LSB due to locally variable basin subsidence, followed by inversion during the Paleogene (Betz et al., 1987, Bruns et al., 2013). The organic matter contained within the Posidonienschiefer has therefore been exposed to vastly different degrees of heating over horizontal distances of tens of kilometers. These characteristics of the Posidonienschiefer deposited in the LSB offer the ideal opportunity to test whether thermal maturation can alter the isotopic composition and concentration of metals contained within organic-rich sedimentary rocks.

Two drilled cores recovered from different parts of the LSB contain ~30-meter-thick stratigraphically equivalent sections of the Posidonienschiefer. These units can be readily correlated to each other via their distinctive enrichments in total organic carbon that stand in contrast to the underlying and overlying organic-poor mudrocks of Pliensbachian/Early Toarcian and Late Toarcian age, respectively (Fig. 2). The units post-date the early Toarcian Oceanic Anoxic Event in the Lower Saxony Basin. One of the Posidonienschiefer successions, in core A, contains labile organic matter with hydrogen indices >700

mgHC/gTOC. By contrast, the organic matter in core B has hydrogen indices of ~0 mgHC/gTOC, demonstrating a substantially greater maximum burial depth, with consequent thermal alteration of organic matter and loss of hydrogen-rich moieties through expulsion of petroleum fluids. The different burial histories of each core are confirmed by reflectance measurements of terrestrial organic macerals (vitrinite, $\%R_o$) of ~0.5 for core A (immature), and ~3.5 for core B (overmature).

METHODS

Element concentrations of samples from cores A and B were measured by first dissolving sample aliquots in a 3:1 mixture of concentrated HNO_3 and HCl at 150–180°C to oxidize organic matter, followed by a 2:1 mixture of HNO_3 and HF at 120°C to dissolve silicates. Measurements were made on sample aliquots diluted in 3% HNO_3 by ICP-MS. Reported concentrations have uncertainties of ±10%, based on replicates of samples, certified reference solutions and materials (SDO-1 USGS shale).

For stable Mo-, Zn-, Cd- and U- isotopes, sample powders were similarly digested completely, after the addition of double-spike solutions (^{100}Mo-^{97}Mo, ^{67}Zn-^{64}Zn, ^{113}Cd-^{111}Cd, ^{236}U-^{233}U). Each element was purified using established anion-exchange methods (Weyer et al., 2008; Dickson et al., 2020; Sweere et al., 2020). Mo-, Zn-, Cd- and U-isotope ratios were measured on a Nu Plasma MC-ICP-MS at the University of Oxford. Isotope ratios are expressed according to the following equation:

$$\left(\left[\frac{(R_{sample}-R_x)}{R_x}\right]\right) * 1000 \quad (1)$$

Where R_{sample} is ^{98}Mo/^{95}Mo, ^{66}Zn/^{64}Zn, ^{114}Cd/^{110}Cd and ^{238}U/^{235}U. R_x is NIST 3134 for Mo, IRMM 3702 for Zn, NIST 3108 for Cd and CRM145 for U. Delta values for Mo and Zn were

105 corrected by 0.25 ‰ and 0.28 ‰, respectively, to place them on their zero-delta scales
106 (Nägler et al., 2014; Archer et al., 2017). External reproducibilities of ±0.08 ‰, ±0.07 ‰ and
107 ±0.06 ‰ (all 2 S.D.) were determined for Mo, Zn and Cd by processing multiple aliquots of
108 USGS SDO-1 through the full analytical procedure. For U, reproducibility was determined
109 from sample replicates and repeated analyses of SRM 950a, giving a value of ±0.1 ‰.
110 Procedural blanks were ~2 ng for Mo, 3 ng for Zn, and <1 ng for Cd and U.
111
112 Hydrogen index (HI) values were measured using a Rock-Eval 6. %TOC data were
113 previously reported in Hooker et al. (2020). Accuracy and precision of the measurements
114 were quantified with an internal shale standard (St Audries Bay Shale) as ±0.2 % for %TOC
115 and ±15 mgHC/gTOC for HI. Highly reactive Fe species (Fe_{HR}) were determined with
116 established techniques (Poulton and Canfield, 2005). Replicate AAS analyses gave a RSD
117 of <5% for all extraction steps. Total Fe concentrations (Fe_T) used to calculate Fe_{HR}/Fe_T
118 ratios were determined by XRF with uncertainties determined from replicate standards, of
119 <1%.
120
121 **RESULTS AND DISCUSSION**
122 **Metal Geochemistry of Immature and Over-Mature Deposits**
123 The mean isotopic compositions of Mo, U, Zn and Cd in bulk-rock analyses of the
124 Posidonienschiefer in cores A and B are the same within the associated uncertainties of the
125 methods (Fig. 3). Despite the fact that the two sedimentary successions are conservatively
126 correlated together (Fig. 2), stratigraphic profiles of the Mo-, U-, Zn- and Cd-isotope datasets
127 are also similar. *t*-tests of all four populations of isotope data from within the
128 Posidonienschiefer interval do not allow a null hypothesis, namely that the data are identical,
129 to be rejected at >95% significance (Table 1). Slight differences in isotopic compositions

stratigraphically above and below the Posidonienschiefer are probably related to the lower non-detrital concentrations of the elements in these deposits.

The similarity of the isotopic compositions of Mo, U, Zn and Cd in the immature and overmature successions of cores A and B suggests either that these metals can be released during thermally induced bond-reorganization and subsequently become re-fixed with residual kerogen / pyro-bitumen or to inorganic minerals (e.g. pyrite). Alternatively, they may be mostly inorganically bound within the mudrock matrix. Laboratory experiments are consistent with these mechanisms by showing that a high fraction of the metal inventory of pyrolyzed Posidonienschiefer rocks resides within a non-extractable phase (Dickson et al., 2020). The mobilization of a significant fraction of metals to organic fluids during secondary migration is not supported by either the high concentrations of Mo, U, Zn and Cd in the overmature deposits of core B (Fig. 3), or by the low abundances of these metals that have been measured in organic fluids produced during pyrolysis-induced thermal cracking and in natural oils (Odermatt and Curiale, 1991; Ventura et al., 2015; Dickson et al., 2020).

The mean concentrations of Mo, U, Zn and Cd are consistently higher in core B than in core A (Fig. 3). The magnitudes of these differences are 45% for Mo, 185% for U, 22% for Zn and 10% for Cd, which are similar to increases in metal concentrations observed in the residues of artificially pyrolyzed rock samples (6–57% for Mo, 21–52% for Zn and 15–19% for Cd) (Dickson et al., 2020). Stratigraphic variability in the down-core profiles of the metals, however, means that the populations of concentration data are only significantly different (>95%) for Mo and U (Table 1).

The LSB contains active petroleum systems, for which the Posidonienschiefer is a major source rock (Kockel et al., 1994). During catagenesis, source rocks with Type II kerogen

156 can lose >30–40% of their original organic matter due to cracking and secondary migration
157 (Raiswell and Berner, 1987), which is similar to previous estimates of organic-carbon loss
158 from mature Posidonienschiefer successions in northern Germany (Littke et al., 1991). The
159 differences in metal concentrations between core A and core B can be linked to the loss of
160 substrate mass caused by the secondary migration of organic fluids, but with a smaller loss
161 of metals. This interpretation is consistent with the limited isotopic differences between the
162 two cores, which point to the retention of metals within the thermally altered rocks in core B.
163
164 The attribution of geochemical differences (or lack thereof) between cores A and B to
165 contrasting thermal histories requires that the original depositional conditions at the two
166 locations were the same. The long residence times of Mo, U, Zn and Cd (10,000–500,000
167 years in the modern ocean, Ku et al., 1977; Bruland, 1980; Miller et al., 2011; Little et al.,
168 2013), imply that their isotopic compositions in seawater (deep ocean for Cd and Zn) would
169 be near homogenous. Even if the marginal marine basins of the Early Jurassic
170 epicontinental European shelf sea experienced a ~10-fold decrease in trace-metal
171 concentrations similar in magnitude to estimates for Cretaceous Oceanic Anoxic Event 2
172 (Owens et al., 2016), seawater values are still unlikely to have decreased by enough to
173 cause isotopic heterogeneity *within* the LSB waters that would be resolvable between the
174 two core locations.
175
176 Small differences in paleo-depositional conditions may, however, have influenced trace-
177 metal concentrations. Both cores contain similar thicknesses of the Posidonienschiefer (~30
178 m) that indicates a first-order similarity in accumulation rates. However, core A contains
179 higher concentrations of detrital elements such as Al and Ti than core B, suggesting that it
180 was deposited in a more proximal setting (Fig. S1). Similarly, the concentration of organic
181 carbon in core B is only slightly less than in core A, despite the fact that a large amount of

182 'original' organic matter may have been lost as migrated hydrocarbons during maturation
183 (Raiswell and Berner, 1987). A higher original %TOC for core B than core A (i.e. >15%)
184 would account for this observation and would support the contention that core B was located
185 in a more distal, perhaps more subsident and deeper water, part of the LSB where the
186 potential for accumulation of organic matter was greater. Slightly higher metal accumulation
187 rates, coupled with less dilution by detrital phases in the deeper parts of the LSB, may thus
188 have contributed to the difference in metal concentrations between the two cores. The slight
189 differences in paleo-depositional conditions are supported by basin modelling (Bruns et al.,
190 2013) and explain why metal/TOC ratios in core B overlap with metal/TOC ratios in core A
191 (Fig. S2). Nonetheless, higher average metal/TOC ratios in core B, particularly for Mo and
192 U, are consistent with laboratory experiments that indicate percent level increases in
193 metal/TOC ratios with increasing maturity. These changes probably occurred due to the loss
194 of organic matter with a low metal content during secondary migration (Dickson et al., 2020).
195 In thermally altered mudrocks, these ratios are therefore maximum estimates of their syn-
196 depositional values.
197
198 **Isotopic Constraints on the Composition of Early Jurassic Seawater**
199 Preservation of the isotopic composition of metals in the ~182 Ma Posidonienschiefer allows
200 the corresponding values in seawater in the LSB to be constrained. Fe-speciation data (Fig.
201 1) suggest that the entire shale unit was deposited under euxinic conditions. Cross-plots of
202 Cd/Mo versus Mn*Co (Sweere et al., 2016) support a depositional environment similar to
203 the modern Black Sea (Fig. S3), where the isotopic compositions of Cd, Zn and Mo are
204 similar to the global deep ocean (Neubert et al., 2008; Vance et al., 2016; Bryan, 2018).
205 Thus, the isotopic compositions of these elements in LSB seawater were close to ~0.07 ±
206 0.13 ‰, ~0.58 ± 0.20 ‰ and ~1.70 ± 0.42 ‰, respectively (average and 2 S.D. of Cores A
207 and B). U isotopes in shales are dominated by the burial of isotopically heavy U(IV) that is

offset from coeval seawater by ~+0.6 ‰ (Andersen et al., 2014): the average of the Posidonienschiefer samples (0.09 ± 0.23 ‰) therefore equates to a LSB seawater estimate of ~-0.5 ‰. The reconstructed Zn-isotope composition of LSB seawater overlaps with that of the modern deep ocean, unlike the Cd-, Mo- and U-isotope values that are all lower.

The very low Cd-isotope value is close to that of the Bulk Silicate Earth (~0 ‰, Schmitt et al., 2009). Biological fractionation in the upper ocean would have increased the Cd-isotope composition of water entering the LSB across a shallow sill, so such a mechanism cannot explain these low values. Likewise, there is no isotopically heavy removal sink for Cd in the oceans that could produce such low values. The large-scale burial of Cd into marine sediments globally could move the oceanic composition close to that of the weathering input fluxes but would require a large change in global Cd cycling that cannot be resolved from the LSB data alone. The inferred LSB seawater Mo-isotope composition is probably a minimum estimate, given that sediments accumulating in some euxinic basins may be offset from coeval seawater by -0.5 to -0.7 ‰ (Dickson, 2017). Nonetheless, the LSB value is consistent with data from similar-age shales in southern Germany, the Netherlands and Yorkshire, UK (Dickson et al., 2017). The U-isotope composition of LSB seawater probably reflects a slightly greater burial flux of U(VI) into marine sediments in the Early Jurassic compared to the modern situation.

CONCLUSIONS

A recent study found limited isotopic variation in Mo, Zn and Cd during laboratory pyrolysis of organic-rich rocks, while finding percent-level increases in metal concentrations with maturation (Dickson et al., 2020). However, the rapid laboratory heating rates, compared to geological conditions, make their application to natural systems uncertain. The new data from the LSB confirm the relevance of these findings to natural systems, despite the

234 significantly different timescales (millions of years versus weeks) and magnitudes (tens of
235 °C versus hundreds of °C) of heating in each situation. Importantly, the new data
236 demonstrate that metal-isotope compositions in organic-rich rocks are not significantly
237 affected by thermal alteration of organic matter in the host substrate, and thus retain primary
238 paleo-chemical information. By contrast, metal concentrations may be elevated above their
239 syn-depositional values in highly mature rocks, thus giving maximum constraints on the
240 concentrations of these elements in ancient sediments.
241

242 **ACKNOWLEDGEMENTS**

243 We thank Daniel Minisini, Matthew Thirlwall, Yu-Te Hsieh and Philip Holdship for assistance
244 with sampling and analyses and Dave Sansom for drafting Fig. 1. The study was funded by
245 Shell Global Solutions International B.V. ExxonMobil Production Deutschland GmbH
246 provided access to core material.
247
248
249
250
251
252
253
254
255
256
257
258
259

REFERENCES

Andersen, M.B., Romaniello, S., Vance, D., Little, S.H., Herdman, R. and Lyons, T.W., 2014, A modern framework for the interpretation of $^{238}U/^{235}U$ in studies of ancient ocean redox: Earth and Planetary Science Letters v. 400, 184–194, doi:10.1016/j.epsl.2014.05.051.

Archer, C., Andersen, M.B., Cloquet, C., Conway, T.M., Dong, S., Ellwood, M., Moore, R., Nelson, J., Rehkämper, M., Rouxel, O., Samanta, M., Shin, K-C., Sohrin, Y., Takano, S. and Wasylenki, L., 2017, Inter-calibration of a proposed new primary reference standard AA-ETH Zn for zinc isotope analysis: Journal of Analytical Atomic Spectrometry v. 32, 415–419, doi:10.1039/C6JA00282J.

Betz, D., Fürher, F., Greiner, G. and Plein, E., 1987, Evolution of the Lower Saxony Basin: Tectonophysics 137, v. 127–170, doi:10.1016/0040-1951(87)90319-2.

Bruns, B., di Primio, R., Berner, U. and Littke, R., 2013, Petroleum system evolution in the inverted Lower Saxony Basin, northwest Germany: a 3D basin modelling study: Geofluids v. 13, 246–271, doi: 10.1111/gfl.12016.

Bruland, K. W., 1980, Oceanographic distributions of cadmium, zinc, nickel, and copper in the north Pacific: Earth and Planetary Science Letters v. 47, 176–198, doi:10.1016/0012-821X(80)90035-7.

Bryan, A.L. (2018), Investigation of the controls on the cadmium isotope composition of modern marine sediments. DPhil thesis, University of Oxford.

Bryan, A.L., Dickson, A.J., Dowdall, F., Homoky, W.B., Porcelli, D. and Henderson, G.M., 2021, Controls on the cadmium isotope composition of modern marine sediments: Earth and Planetary Science Letters v. 565, 116964, doi:10.1016/j.epsl.2021.116946.

Chappaz, A., Lyons, T.W., Gregory, D.D., Reinhard, C.T., Gill, B.C., Li, C. and Large, R.R., 2014, Does pyrite act as an important host for molybdenum in modern and ancient euxinic sediments?: Geochimica et Cosmochimica Acta v. 126, 112–122, doi:10.1016/j.gca.2013.10.028.

Clarkson, M.O., Stirling, C.H., Jenkyns, H.C., Dickson, A.J., Porcelli, D., Moy, C.M., Pogge von Strandmann, P.A.E., Cooke, I.R. and Lenton, T.M., 2018, Uranium isotope evidence for two episodes of deoxygenation during Oceanic Anoxic Event 2: Proceedings of the National Academy of Sciences v. 115, 2918–2923, doi:10.1073/pnas.1715278115.

Dahl, T.W., Chappaz, A., Hoek, J., McKenzie, C.J., Svane, S. and Canfield, D.E., 2017, Evidence of molybdenum association with particulate organic matter under sulfidic conditions: Geobiology v. 15, 311–323, doi:10.111/gbl.12220.

Dickson, A.J., 2017, A molybdenum isotope perspective on Phanerozoic deoxygenation events. Nature Geoscience v. 10, 721–726, doi:10.1038/ngeo3028.

Dickson, A.J., Idiz, E., Porcelli, D. and van den Boorn, S.H.J.M., 2020, The influence of thermal maturity on the concentrations and isotopic compositions of Mo, Zn and Cd in organic-rich marine mudrocks: Geochimica et Cosmochimica Acta v. 287, 205–220, doi: 10.1016/j.gca.2019.11.001.

Eroglu, S., Scholz, F., Salvatteci, R., Siebert, C., Schneider, R. and Frank, M., 2021, The impact of postdepositional alteration on iron- and molybdenum-based redox proxies: Geology, doi:10.1130/G49291.1.

Georgiev, S.V., Horner, T.J., Stein, H.J., Hannah, J.L., Bingen, B. and Rehkämper, M., 2015, Cadmium-isotopic evidence for increasing primary productivity during the Late Permian anoxic event: Earth and Planetary Science Letters v. 410, 84–96, doi:10.1016/j.epsl.2014.11.010.

Hooker, J.N., Ruhl, M., Dickson, A.J., Hansen, L.N., Idiz, E., Hesselbo, S.P. and Cartwright, J., 2020, Shale anisotropy and natural hydraulic fracture propagation: and example from the Jurassic (Toarcian) Posidonienschiefer, Germany: Journal of Geophysical Research: Solid Earth v. 125, doi:10.1029/2019JB018442.

Isson, T.T., Love, G.D., Dupont, C.L., Reinhard, C.T., Zumberge, A.J., Asael, D., Gueguen, B., McCrow, J., Gill, B.C., Owens, J., Rainbird, R.H., Rooney, A.D., Zhao, M-Y., Steeuken, E.E., Konhauser, K.O., John, S.G., Lyons, T.W. and Planavsky, N.J., 2018, Tracking the rise of eukaryotes to ecological dominance with zinc isotopes: Geobiology v. 16, 341–352, doi:10.1111/gbi.12289.

Kockel, F., Wehner, H. and Gerling, P., 1994, Petroleum systems of the Lower Saxony Basin, Germany, in Magoon, L.B., and Dow, D.G., eds., The petroleum system—from source to trap: AAPG Memoir 60, p. 573–586, doi:10.1306/M60585C34.

337 Ku, T.L., Knauss, K.G. and Mathieu, G.G., 1977, Uranium in open ocean – concentration,
338 and isotopic composition: Deep-Sea Research v. 24, 1005–1017, doi:10.1016/0146-
339 6261(77)90571-9.
340
341 Lewan, M.D. and Maynard, J.B., 1982, Factors controlling enrichment of vanadium and
342 nickel in the bitumen of sedimentary rock: Geochimica et Cosmochimica Acta v. 46, 2547–
343 2560, doi: 10.1016/0016-7037(82)90377-5.
344
345 Littke, R., Baker, D.R., Leythaeuser, D. and Rullkötter, J., 1991, Keys to the depositional
346 history of the Posidonienschiefer (Toarcian) in the Hils Syncline, northern Germany, in
347 Tyson, R.V. and Pearson, T.H., eds., Modern and ancient continental shelf anoxia:
348 Geological Society Special Publication 58, p. 311–333.
349
350 Little, S.H., Vance, D., McManus, J. and Severmann, S., 2016, Key role of continental
351 margin sediments in the oceanic mass balance of Zn and Zn isotopes: Geology v. 44, 207–
352 210, doi:10.1130/G37493.1.
353
354 Little, S.H., Vance, D., Walker-Brown, C. and Landing, W.M., 2013, The oceanic mass
355 balance of copper and zinc isotopes, investigated by analysis of their inputs, and outputs to
356 ferromanganese oxide sediments: Geochimica et Cosmochimica Acta v. 125, 673–693,
357 doi:10.1016/j.gca.2013.07.046.
358
359 Miller, C.A., Peucker-Ehrenbrink, B., Walker, B.D. and Marcantonio, F., 2011, Re-assessing
360 the surface cycling of molybdenum and rhenium: Geochimica et Cosmochimica Acta v. 75,
361 7146–7179, doi:10.1016/j.gca.2011.09.005..
362

363 Nägler, T.F., Anbar, A.D., Archer, C., Goldberg, T., Gordon, G.W., Greber, N.D., Siebert, C.,
364 Sohrin, Y. and Vance, D., 2014, Proposal for an international molybdenum isotope
365 measurement standard and data representation: Geostandards and Geoanalytical
366 Research v. 38, 149–151, doi:10.1111/j.1751-908X.2013.00275.x.
367
368 Neubert, N., Nägler, T.F. and Böttcher, M.E. (2008) Sulfidity controls molybdenum isotope
369 fractionation into euxinic sediments: evidence from the modern Black Sea. Geology v. 36,
370 775–778, doi:10.1130/G24959A.1.
371
372 Odermatt, J.R. and Curiale, J.A., 1991, Organically bound metals and biomarkers in the
373 Monterey Formation of the Santa Maria Basin, California: Chemical Geology v. 91, 99–113,
374 doi:10.1016/0009-2541(91)90084-5.
375
376 Owens, J.D., Reinhard, C.T., Rohrssen, M., Love, G.D. and Lyons, T.W., 2016, Empirical
377 links between trace metal cycling and marine microbial ecology during a large perturbation
378 to Earth's carbon cycle: Earth and Planetary Science Letters v. 449, 407–417,
379 doi:10.1016/j.epsl.2016.05.046.
380
381 Poulton, S.W. and Canfield, D.E., 2005, Development of a sequential extraction procedure
382 for iron: implications for iron partitioning in continentally derived particulates: Chemical
383 Geology v. 214, 209–221, doi:10.1016/j.chemgeo.2004.09.003.
384
385 Raiswell, R. and Berner, R.A., 1987, Organic carbon losses during burial and thermal
386 maturation of normal marine shales: Geology v. 15, 853–856, doi:10.1130/0091-
387 7613(1987)15<853:OCLDBA>2.0.CO;2.
388

389 Schmitt, A-D., Galer, S.J.G. and Abouchami, W., 2009, Mass-dependent cadmium isotopic
390 variations in nature with emphasis on the marine environment: Earth and Planetary Science
391 Letters v. 277, 262–272, doi:10.1016/j.epsl.2008.10.025.
392
393 Sweere, T.C., Dickson, A.J., Jenkyns, H.C., Porcelli, D., Ruhl, M., Murphy, M.J., Idiz, E., van
394 den Boorn, S.H.J.M., Eldrett, J.S. and Henderson, G.M., 2020, Controls on the Cd-isotope
395 composition of Upper Cretaceous (Cenomanian–Turonian) organic-rich mudrocks from
396 South Texas (Eagle Ford Group): Geochimica et Cosmochimica Acta v. 287, 251–262,
397 doi:10.1016/j.gca.2020.02.019.
398
399 Sweere, T., van den Boorn, S., Dickson, A.J. and Reichart, G-J., 2016, Definition of new
400 trace-metal proxies for the controls on organic matter enrichment in marine sediments based
401 on Mn, Co, Mo and Cd concentrations: Chemical Geology v. 441, 235–245,
402 doi:10.1016/j.chemgeo.2016.08.028.
403
404 Vance, D., Little, S.H., Archer, C., Cameron, V., Andersen, M.B., Rijkenberg, M.J.A. and
405 Lyons, T.W., 2016, The oceanic budgets of nickel and zinc isotopes: the importance of
406 sulfidic environments as illustrated by the Black Sea: Philosophical Transactions of the
407 Royal Society v. A374, 20150294, doi:10.1098/rsta.2015.0294.
408
409 Ventura, G.T., Gall, L., Siebert, C., Prytulak, J., Szatmari, P., Hürlimann, M., Halliday, A.N.
410 (2015) The stable isotope composition of vanadium, nickel, and molybdenum in crude oils.
411 Applied Geochemistry 59, 104–117, doi:10.1016/j.apgeochem.2015.04.009.
412
413 Weyer, S., Anbar, A.D., Gerdes, A., Gordon, G.W., Algeo, T.W., Boyle, E.A. (2008) Natural
414 fractionation of $^{238}U/^{235}U$. Geochimica et Cosmochimica Acta 72, 345–359.

Figure captions

Figure 1: Location of the Lower Saxony Basin (LSB) in the Early Jurassic (c. 180 Ma). Modern shorelines are shown as dashed lines.

Figure 2: Stratigraphy of core A (circles) and core B (squares). Core B has been placed on the depth scale of core A by identifying tie-points (arrows) at the top and bottom of the organic-rich interval and at the peak in Mo concentrations in the lower part of the unit (shown in Fig. 3), and linearly interpolating depths between these tie-points. The horizontal dashed lines indicate the stratigraphic position of the Posidonienschiefer.

Figure 3: Metal geochemical profiles for core A (circles) and core B (squares). Core B is plotted on the core A depth scale, as defined in Fig. 1. The 2 S.D. external reproducibilities for each isotope system are shown by horizontal bars.

Variable	**Core A**			**Core B**				
	Mean	**Standard deviation**	**No. observations**	**Mean**	**Standard deviation**	**No. observations**	***t*-value**	***p*-value**
TOC, %	10.6	2.2	31	9.5	1.9	32	2.177	0.033
HI	694	22	31	3	4	32	168.26	<0.0001
[Mo], ppm	70.5	39.9	31	101.9	52.3	31	-2.66	0.010
$\delta^{98/95}$Mo	1.67	0.22	31	1.70	0.22	31	-0.608	0.545
[Zn], ppm	178	97	15	217	80	13	-1.165	0.255
$\delta^{66/64}$Zn	0.58	0.11	15	0.59	0.10	12	-0.372	0.713
[Cd], ppm	1.7	1.1	17	1.8	0.6	15	-0.524	0.605
$\delta^{114/110}$Cd	0.02	0.17	14	0.05	0.09	13	-0.558	0.583
[U], ppm	5.7	2.4	15	16.1	11.8	10	-2.777	0.021
$\delta^{238/235}$U	0.08	0.09	15	0.12	0.12	11	-1.016	0.323

Table 1: t-test results. Variables for which the null hypothesis (no difference between Core A and B) can be rejected at >95% significance are italicized.

436 Figure 1

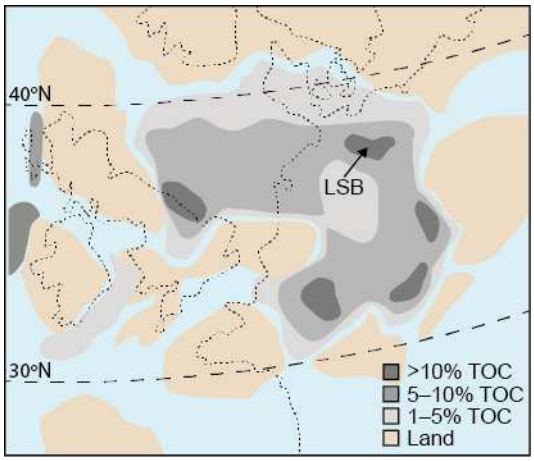

437

438

439 Figure 2

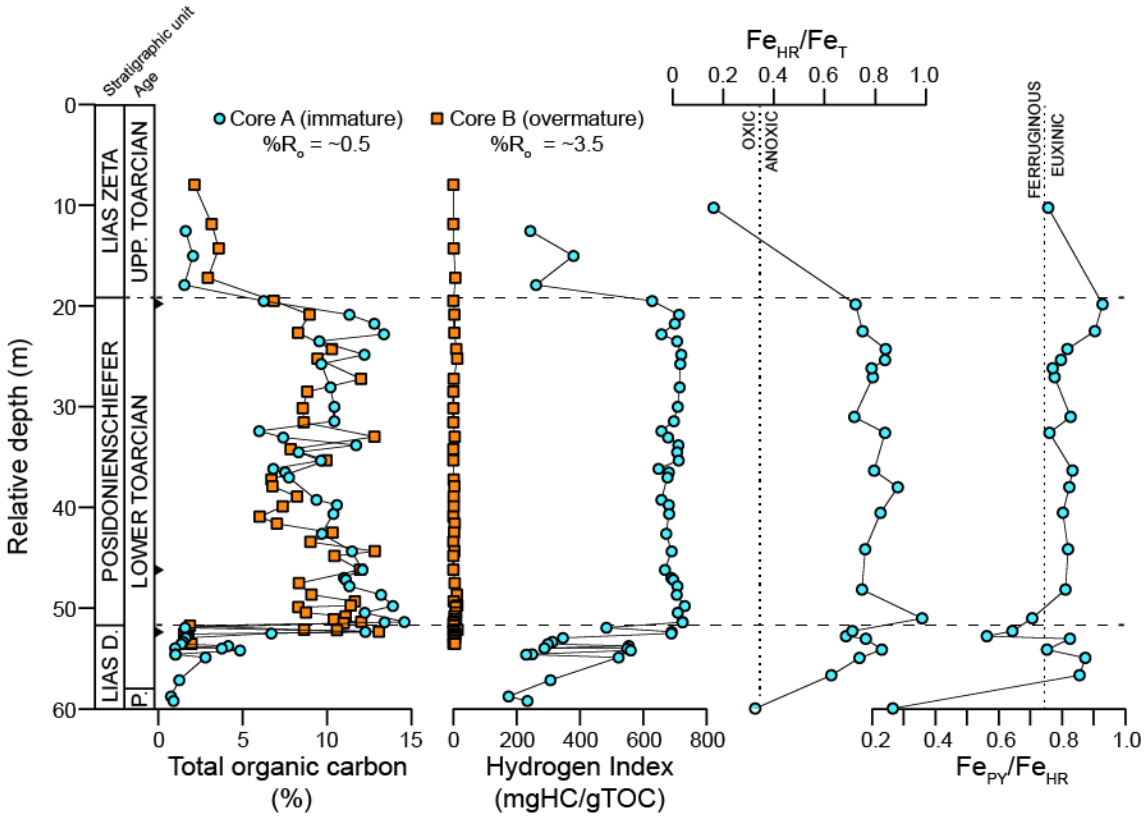

440

441

442

443

444

445 Figure 3

446

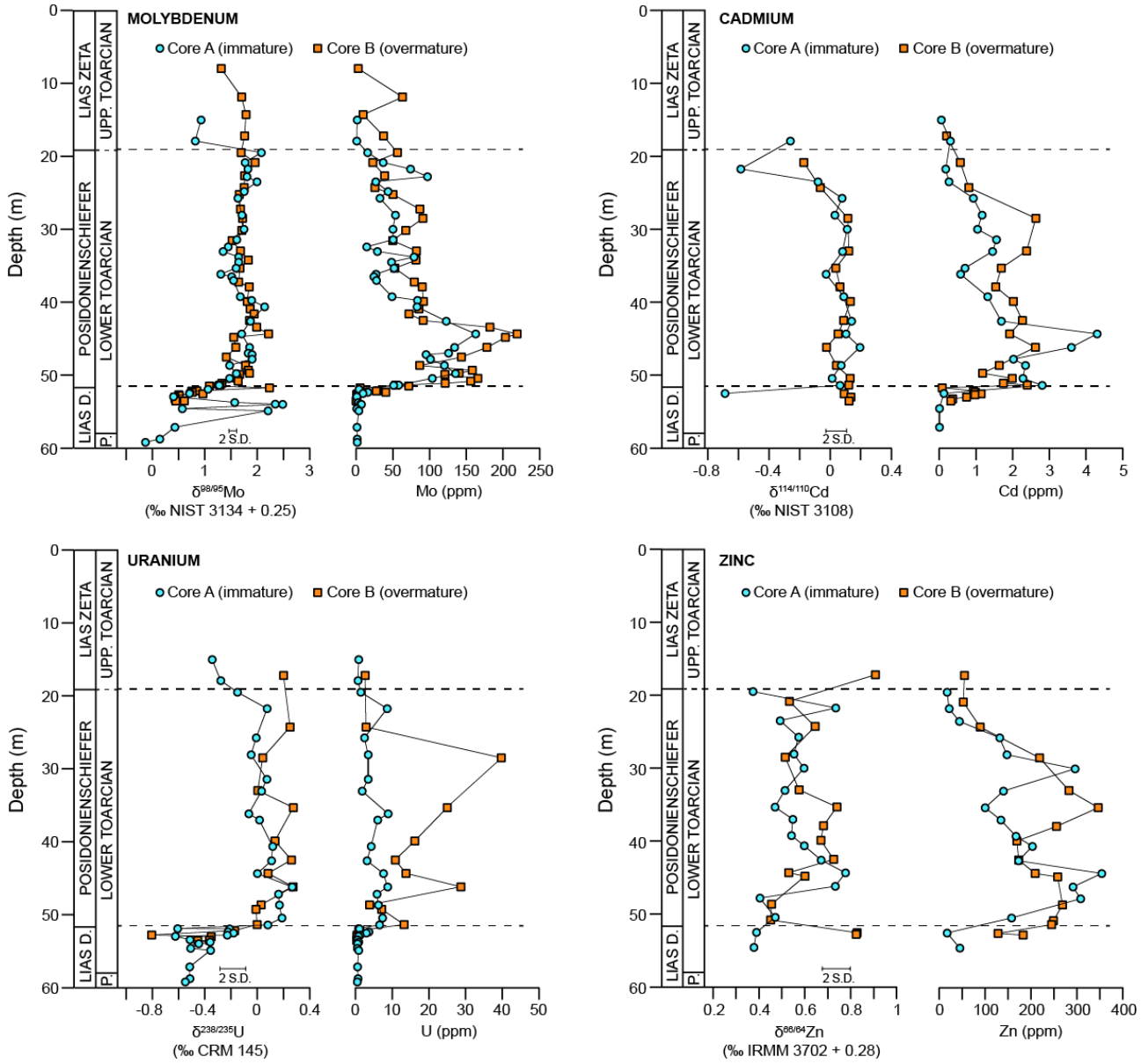

447

448

449